ACS Catalysis

pubs.acs.org/acscatalysis

Research Article

Adjusting the Chemical Reactivity of Oxygen for Propylene Epoxidation on Silver by Rational Design: The Use of an Oxyanion and Cl

Emilia A. Carbonio,* Frederic Sulzmann, Alexander Yu. Klyushin, Michael Hävecker, Simone Piccinin, Axel Knop-Gericke, Robert Schlögl, and Travis E. Jones*

Cite This: *ACS Catal.* 2023, 13, 5906−5913

Read Online

ACCESS | Metrics & More | Article Recommendations | Supporting Information

ABSTRACT: The development of catalysts for propylene oxide production from direct epoxidation using propylene and oxygen remains a challenge. Compared to ethylene epoxidation, where selectivity on silver catalysts is high, the low selectivity to produce propylene oxide over silver is partially attributed to the lack of electrophilic oxygen under propylene epoxidation reaction conditions. Here, we investigate how to mediate the chemical reactivity of oxygen by theory-inspired experiments for propylene epoxidation. We show how adding electrophilic-O via SO_4 oxyanions to the surface of silver increases epoxide selectivity. Moreover, we show how the addition of Cl to the SO_4-modified catalyst activates the oxyanion, giving a more than 4-fold increase in selectivity to propylene oxide. Finally, we explore different systems using DFT and draw a picture on how the next catalyst/co-catalyst systems should be tuned to design a catalyst with high selectivity for direct propylene oxidation.

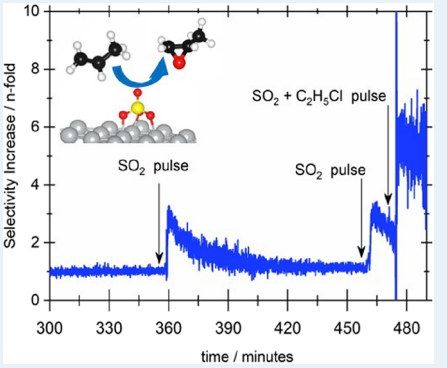

KEYWORDS: *silver, propylene epoxidation, chlorine, sulfur, NAP-XPS, operando*

INTRODUCTION

Alkene epoxidations are an important class of reactions that continue to attract considerable academic and industrial interest.[1−3] A longstanding challenge is the development of catalysts for the direct epoxidation of propylene to propylene oxide (PO) under O_2. Industrially, PO is an important feedstock whose production has a large economic and environmental footprint owing to the continued reliance on chlorohydrin processes.[2,4] Also, while a hydrogen peroxide to propylene oxide process has been gaining market share, direct gas-phase epoxidation of propylene is still preferable.[4] From an academic standpoint, the lack of effective catalysts for this process is intriguing, as the C_2 epoxide, ethylene oxide, is readily formed through the reaction of ethylene and oxygen over silver. This difference in reactivity is attributed to the presence of a labile allylic C−H bond in propylene.[5] Circumventing H abstraction during propylene epoxidation then requires a highly selective catalyst. In this work, we employed recent insights from the catalytic chemistry of ethylene epoxidation and Density Functional Theory (DFT) calculations to predictably increase the selectivity of silver toward propylene epoxidation. We go on to verify the origins of these changes using *operando* X-ray photoelectron spectroscopy (XPS).

Studies of ethylene epoxidation have shown that epoxide selectivity is mediated by the nature of the oxygen species present on the catalyst surface, where two broad classes of oxygen are discernable by XPS, nucleophilic (O_{nuc}), and electrophilic (O_{elec}) oxygen. O_{elec} is a class of covalently bound oxygen[6−8] and is the only species known to participate in epoxidation.[8,9] O_{nuc} is a class of oxygen induced surface reconstructions that, while active only in combustion, is required to activate O_{elec}.[8,10] During epoxidation, the formation of the selective O_{elec} requires high near-surface oxygen concentrations,[8,9] which are difficult to achieve during propylene epoxidation owing to the high reducing potential of propylene.[11] Thus, the lack of O_{elec} may be a limitation in the direct epoxidation of propylene on silver,[11] but this has yet to be proven. While increasing the concentration of O_{elec} may improve propylene oxide selectivity, the nature of this species, and hence means of increasing its coverage, has been long debated.[2,9,12−15] In early investigations it was postulated that a special form of adsorbed oxygen (O_{ads}) would selectively oxidize ethylene to EO.[16−18] In propylene oxidation, facile allylic hydrogen abstraction by O_{ads} results in either complete combustion or acrolein formation.[19] It was proposed that

Received: January 19, 2023
Revised: March 15, 2023
Published: April 17, 2023

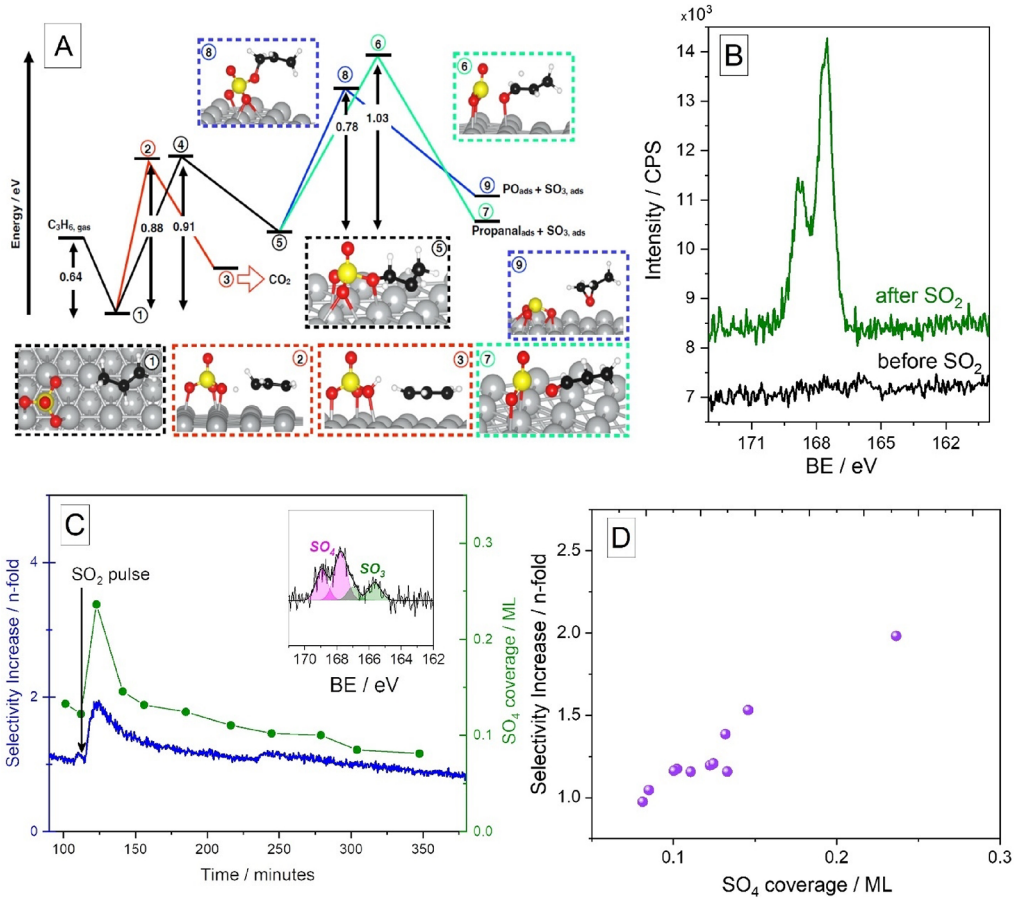

Figure 1. (A) Minimum energy paths for the reaction of propylene with $SO_{4,ads}$ on the unreconstructed silver surface. Propylene adsorption and allyl-H abstraction path (2,3), SO_3−O−C_3H_6 formation intermediate (4), SO_3−O−C_3H_6 state (5), PA intermediate and formation (6,7), and PO intermediate and formation (8,9). (B) S 2p before and after a SO_2 pulse for a Ag pellet under 2:1 O_2:C_3H_6 at 230 °C and 0.5 mbar, (C) PO selectivity increase (determined from QMS data) and SO_4 coverage vs time (inset: S 2p after SO_2 pulse showing $SO_{3,ads}$ transient), and (D) PO selectivity increase vs SO_4 coverage.

because propylene is a more effective reducing agent than ethylene, this would inhibit surface-to-subsurface transport of O atoms[11] and the lower epoxide selectivity to PO would result from the weakly electrophilic O_{ads}.[11] However, O_{ads} on silver was recently shown to be incompatible with the spectroscopic measurements of O_{elec},[7,13,20] the only species that has been shown to produce EO.[8,9]

Recently, it was demonstrated that the methods used to prepare O_{elec} on silver lead to the accumulation of a SO_4-(7 × $\sqrt{3}$)rect surface reconstruction, due to sulfur impurities in ethylene and/or silver.[9] A complete characterization of the SO_4-(7 × $\sqrt{3}$)rect surface reconstruction can be found in previous publications.[9,21] The SO_4-(7 × $\sqrt{3}$)rect phase was predicted by DFT to be inactive for ethylene epoxidation due to the high activation energy associated to its direct reaction with ethylene to form a C−O bond.[9] However, the formation of O-induced surface reconstructions was shown to partially lift the inactive SO_4-(7 × $\sqrt{3}$)rect surface reconstruction and form a metastable adsorbed-SO_4 ($SO_{4,ads}$). $SO_{4,ads}$ was shown to make EO in TPR and to improve EO-production under reaction conditions using NAP-XPS,[9] and $SO_{4,ads}$ was demonstrated to have the spectroscopic properties associated with O_{elec}.[9] It was concluded that O_{elec} is the oxygen in $SO_{4,ads}$ formed as a result of trace sulfur impurities.[9] This recent development in ethylene epoxidation on silver led us to investigate this sulfur species in direct propylene epoxidation on silver. With the identification of the nature of O_{elec}, it becomes possible to investigate the possible role of $SO_{4,ads}$ in propylene epoxidation over silver. To do so, we have used DFT calculations and *operando* NAP-XPS measurements.

RESULTS

Figure 1A shows the results of minimum-energy-path (MEP) calculations performed for the reaction of $SO_{4,ads}$ with propylene on Ag(111). Critically, $SO_{4,ads}$ does not selectively activate the allylic C−H bond of propylene—unlike the strongly nucleophilic atomic O[19,22,23] that participates in allylic-H abstraction. Instead, Figure 1A shows that the activation energy associated with allyl formation is competitive with the formation of a SO_3−O−C_3H_6 intermediate. Unlike allyl formation, which leads to combustion, the formation of the SO_3−O−C_3H_6 is predicted to lead to the partial oxidation of propylene to PO and to a less extent to propanal (PA) in a manner analogous to ethylene epoxidation. Also, as in the case of ethylene epoxidation, the V+ oxidation state of $SO_{4,ads}$ facilitates ring closure resulting in selective PO formation. Thus, the MEPs predict a PO selectivity of *ca.* 50% could be reached through the reaction of propylene with electrophilic oxygen ($SO_{4,ads}$) on silver.

To experimentally test the hypothesis that an increase in O_{elec} will improve PO selectivity, we turned to *operando* XPS. Here, we use NAP-XPS to investigate a silver powder catalyst

https://doi.org/10.1021/acscatal.3c00297
ACS Catal. 2023, 13, 5906−5913

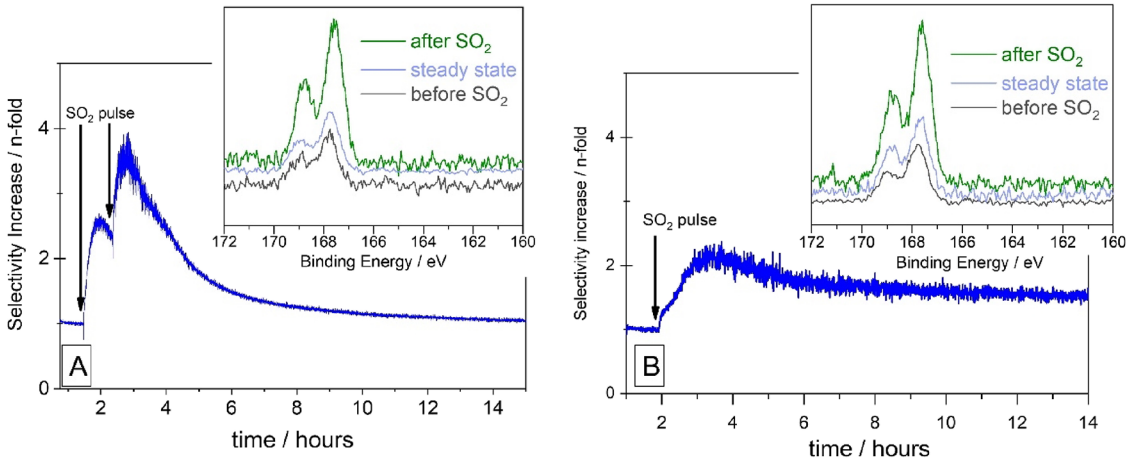

Figure 2. Selectivity increase on a Ag pellet obtained for SO_2 pulsing into the reaction feed of (A) 5:1 O_2:C_3H_6 and (B) 10:1 O_2:C_3H_6, at 230 °C and 0.5 mbar, estimated with online QMS. Insets: S2p measured under the reaction.

under propylene oxidation conditions (O_2:C_3H_6 2:1, at 230−270 °C and 0.3−0.5 mbar total pressure). Figure 1B shows that—unlike under ethylene epoxidation conditions under the same O_2:alkene ratio, where $SO_{4,ads}$ accumulates during the reaction[9]—during propylene oxidation, we find that SO_x-species are present only in negligible amounts (*ca.* 0.1 ML). This finding is in line with the previous observation that an oxygen species consistent with O_{elec} does not accumulate during propylene epoxidation on silver.[11] As discussed below, this absence of O_{elec} is due to the large reductive potential of propylene, and in this state, the catalyst is highly selective to CO_2.

PO selectivity was quantified by way of on-line quadrupole mass spectrometry (QMS) and/or gas chromatography (GC), directly attached to the NAP-XPS chamber (Figure S1), where the former offers higher time resolution. Propylene oxide and carbon dioxide were identified as the main products with both QMS, based on the analysis of mass fragments, and GC, based on the elution time of reaction products compared to certified calibration gases (see SI). With this normal state of the catalyst determined, we can now turn to the role of increasing O_{elec}.

One strategy to create O_{elec} is to introduce oxidized sulfur directly into the gas feed. Here, this was performed through SO_2 pulsing, as SO_2 is known to react with oxygen at the O−Ag surface reconstruction and form SO_4 at temperatures higher than 160 °C.[24] Figure 1B clearly shows that this strategy leads to the formation of SO_4 (identified by its binding energy of 167.4 eV)[9] during propylene epoxidation. In line with the hypothesis that increasing SO_4 will increase the formation of O_{elec} on the silver catalyst, upon SO_2 pulsing, the selectivity to PO increases (Figure 1C). However, selectivity decreases following the SO_2 dose and can be seen to correlate with the consumption of surface SO_4. During the course of this titration, the selectivity to PO can be seen to correlate with the SO_4 amount on the catalyst surface (Figure 1D), as predicted. The titration of SO_4 during propylene oxidation explains why O_{elec} is not seen during normal steady-state epoxidation. In fact, during the titration an $SO_{3,ads}$ species can be seen to form transiently after SO_2 dosing (inset in Figure 1C). Such a species forms when $SO_{4,ads}$ gives an O atom[9] to propylene to form PO (Figure 1A). The accumulation of $SO_{3,ads}$ indicates that further reaction of $SO_{3,ads}$ with propylene is slow. This is supported by MEP calculations of the reaction of $SO_{3,ads}$ with propylene (see SI), which show that while the PO selectivity should be similar to the case of $SO_{4,ads}$, the activation energy for its reaction is 0.1−0.2 eV higher, or *ca.* 10−100 times slower at 500 K assuming Arrhenius behavior with identical prefactors. The continuous loss of S demonstrates reoxidation of $SO_{3,ads}$ is not competitive with its consumption. When considering the low activation energies for reoxidation,[9] we conclude that the slow rate of reoxidation is due to a low coverage of oxygen due to the reductive nature of propylene (see SI). This is in contrast with ethylene epoxidation, where SO_4 coverage remains stable on the Ag surface under the same alkene epoxidation conditions[9] and where higher coverage of oxygen is observed.[25] Here, we would like to point out that both the SO_4-$(7 \times \sqrt{3})$rect and $SO_{4,ads}$ phases are generally present[9] and that the consumption of $SO_{4,ads}$ shifts the equilibrium between these two phases and as a consequence, the inactive SO_4-$(7 \times \sqrt{3})$rect is also consumed (almost) completely.

From the preceding findings, it appears that higher O_2:C_3H_6 ratios would be necessary to facilitate the reoxidation of $SO_{3,ad}$ to $SO_{4,ads}$ during propylene epoxidation. Thus, we performed *operando*XPS experiments using O_2:C_3H_6 5:1 and 10:1 ratios. First, we observe that under these conditions, a higher amount of SO_4 is already present on the catalyst surface without SO_2 dosing (Figure 2). Here, sulfur comes from the oxidation of S traces that are present in propylene[26] and/or silver.[9] The amount of SO_4 still increases upon SO_2 pulsing into the reaction feed. Such pulsing again increases selectivity to PO for both reaction feeds as it did under O_2:C_3H_6 2:1 (Figure 1C). As with the O_2:C_3H_6 2:1 ratio, selectivity is again observed to decrease with time. Though the decrease is slower than for the O_2:C_3H_6 2:1 reaction mixture. In the case of O_2:C_3H_6 5:1, selectivity reaches its initial value after several hours; this change mirrors the drop in the measured SO_4 amount on the catalyst surface (inset Figure 2a). For the O_2:C_3H_6 10:1 reaction feed, selectivity drops slowly with time and even after 12 h it remains higher than the initial selectivity, correlating with the observed SO_4 (inset Figure 2b). In both cases, however, $SO_{3,ads}$ is not observed during selectivity drop, indicating that its reoxidation is more competitive with SO_4 reduction under this condition. These results demonstrate how increased O_2:C_3H_6 ratios likely facilitate $SO_{3,ads}$ reoxidation through increasing the availability of surface oxygen and agree well with O_{elec} being obtained at high near-surface oxygen concentrations[8,9] and being able to maintain the catalyst in a

https://doi.org/10.1021/acscatal.3c00297
ACS Catal. 2023, 13, 5906−5913

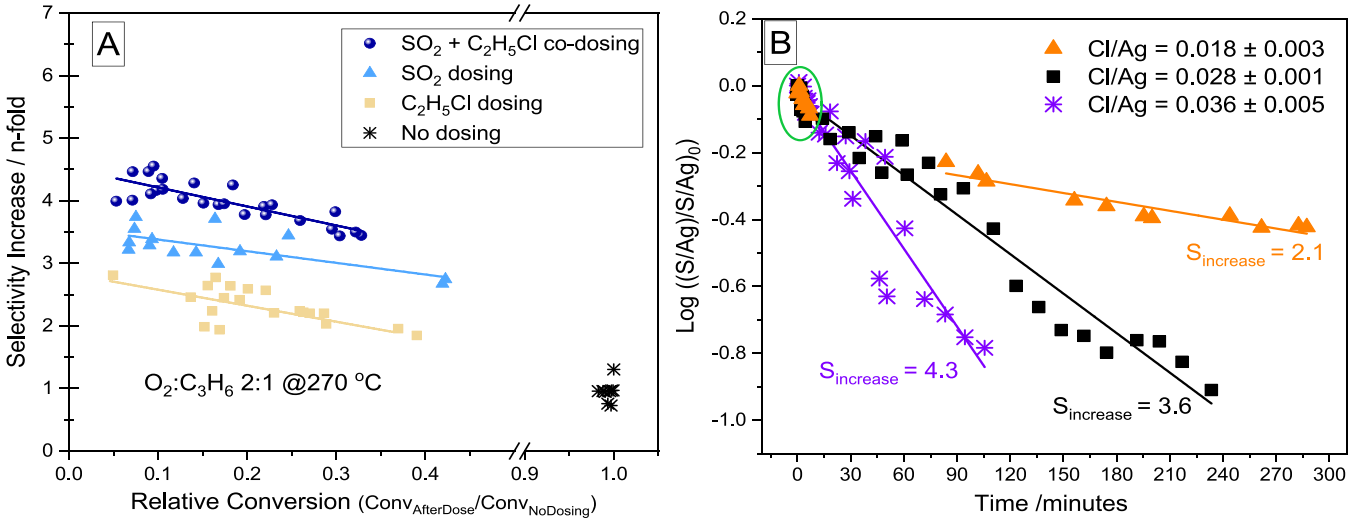

Figure 3. (A) PO selectivity increase for a Ag pellet under 2:1 O_2:C_3H_6 at 270 °C, after C_2H_5Cl-dosing, SO_2-dosing, and SO_2 + C_2H_3Cl co-dosing. (B) Kinetics of SO_4 titration for Cl-containing Ag catalysts with different Cl/Ag ratios (as indicated in the figure), at 230 (orange) and 270 °C (black and purple). The selectivity increase is indicated for each curve.

state of increased selectivity after SO_2 dosing. The details of the reoxidation mechanism of $SO_{3,ads}$ to $SO_{4,ads}$ can be found elsewhere.[9]

A second consequence of the rapid oxygen removal by propylene is that the surface oxygen coverage is low and thus, much of the SO_4 is trapped in the inactive SO_4-$(7 \times \sqrt{3})$rect phase.[9] While Cl_{ads} has a negligible impact on the MEPs (see SI), Cl adsorption is known to induce surface reconstructions on silver,[27−29] such as e.g., Cl-(3×3).[29] Using a Cl co-catalyst is then expected to partially lift the SO_4-$(7 \times \sqrt{3})$rect phase (in an analogous way as for O p-(4×4) surface reconstruction does under ethylene epoxidation)[9] generating $SO_{4,ads}$ without otherwise altering the catalytic chemistry or introducing the reactive O_{nuc} involved in combustion, yielding a means of mediating the $SO_{4,ads}$ coverage that is independent of O_2 pressure. Thus, we evaluated the impact of Cl on the SO_4-containing Ag catalyst.

To test the role of Cl, we compared PO selectivity changes when only SO_4, Cl, or both SO_4 and Cl are added during the NAP-XPS experiments performed under 2:1 O_2:C_3H_6 (by pulses of SO_2 and/or C_2H_5Cl). The amounts of S and Cl on the silver surface were followed by XPS (Figure S2). In the first case, only Cl was added. As before, under 2:1 O_2:C_3H_6 the initial amount of S is small and remains constant during the Cl addition (Figure S2). As expected, introducing Cl increases the PO selectivity (Figure 3A). However, the PO selectivity increase is larger when, instead of C_2H_5Cl, SO_2 is added to increase SO_4 coverage. This behavior is interpreted as an indication that the low surface coverage of SO_4 is limiting PO selectivity when only C_2H_5Cl is dosed, while the SO_4 induced surface reconstruction is problematic when pulsing SO_2. We expect introducing both SO_2 and C_2H_5Cl can then (partially) circumvent both issues.

The highest PO selectivities are found when both SO_2 and C_2H_5Cl are co-dosed during the reaction (Figure 3A), suggesting that the SO_4 induced surface reconstructions are partially lifted by Cl to form the active $SO_{4,ads}$. Thus, co-dosing C_2H_5Cl and SO_2 has the largest effect by activating the SO_4-$(7 \times \sqrt{3})$rect phase and increasing the amount of $SO_{4,ads}$, resulting in a more than 4-fold increase in PO selectivity. In ethylene epoxidation over silver, it is well established that lower conversion gives higher epoxide selectivity.[12,30] It has also been hypothesized that EO production requires smaller Ag ensembles than CO_2 production, allowing Cl to increase epoxide selectivity by reducing the number of those ensembles.[31] Here, we show that introducing $SO_{4,ads}$ to the Ag catalyst has a greater effect than introducing Cl alone, and co-dosing SO_2 and C_2H_5Cl shows even greater selectivity at a given conversion. Thus, the increase in selectivity due to the presence of SO_4, and both SO_4 and Cl on silver, is not due to lower conversion or fewer Ag ensembles alone, but it is intrinsic to the presence of SO_4, which is activated by Cl.

To further test if Cl adsorption can activate the SO_4-induced surface reconstructions, we analyzed the titration kinetics of SO_4 in the presence of different amounts of Cl (Figure 3B). Right after a SO_2 pulse, SO_4 decreases quickly (green circle in Figure 3B) independent of Cl concentration (Table S1). Afterward, we find that SO_4 is titrated faster at a higher Cl/Ag ratio following a rate law of apparent first order, with increasing apparent rate constants, k', for the increasing Cl/Ag, respectively (Table S1). Moreover, the selectivity increase is higher for higher amounts of Cl. This result agrees with Cl-induced surface reconstruction lifting the inactive SO_4-$(7 \times \sqrt{3})$rect phase, thus shifting the equilibrium between the SO_4-$(7 \times \sqrt{3})$rect phase and $SO_{4,ads}$ species, leading to higher concentration of the more reactive and selective $SO_{4,ads}$ species. To understand the initial fast decrease in SO_4 independent of Cl concentration, we explore the impact of higher local $SO_{4,ads}$ coverages (that could be induced during an SO_2 pulse). Although the MEPs for local higher $SO_{4,ads}$ coverages of allyl-H abstraction and SO_3−O−C_3H_6 formation are not significantly altered, the MEPs for the reaction path from the SO_3−O−C_3H_6 to PA and PO are largely reduced at the highest coverage (Table S2; see $SO_{4,ad}$, $2SO_{4,ads}$, and $3SO_{4,ads}$), which would be in agreement with a higher apparent rate constant (Table S1).

With an understanding of the role of $SO_{4,ads}$ on PO selectivity over silver, we sought to understand if this combination is unique or if other co-catalysts or substrates could offer similar performance. From Figure 1, the maximum PO selectivity through the reaction of propylene and $SO_{4,ads}$ can be seen to be mediated by two branching points: (i) the

https://doi.org/10.1021/acscatal.3c00297
ACS Catal. 2023, 13, 5906−5913

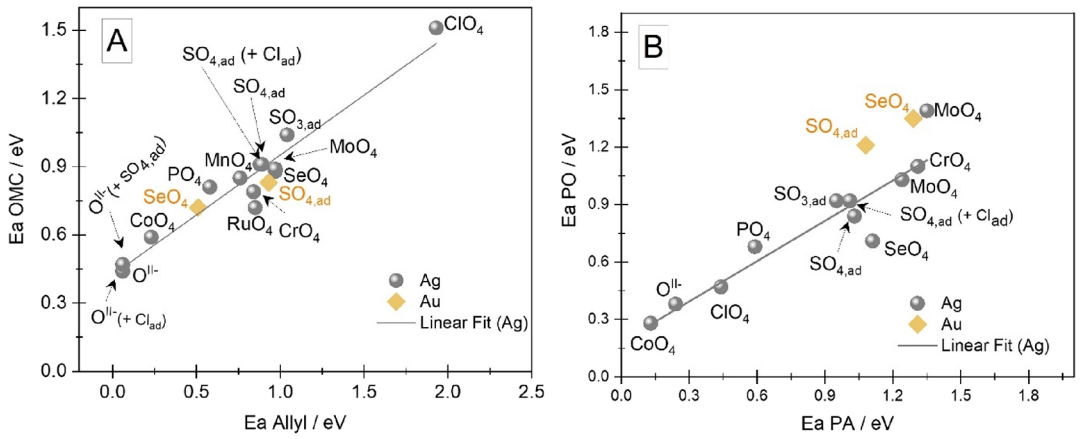

Figure 4. Plots of (A) E_a for the formation of the $XO_3-O-C_3H_6$ intermediate vs C−H bond activation and (B) E_a for PO vs PA formation, over Ag and Au (see Figure 1 for reaction paths).

competition between C−H bond activation and $SO_3-O-C_3H_6$ formation and (ii) the decomposition of the $SO_3-O-C_3H_6$ intermediate. To understand how the chemistry of the oxyanion influences these branching points, we computed the analogous MEPs using a range of oxyanions. Because the first branching point is expected to be tied to basicity,[22] we chose oxyanions with pkB's ranging from *ca.* 2 to 20 (XO_4, X = Cl, Co, Cr, Mn, Mo, P, Ru, Se, S). We find that the activation energies for C−H bond activation and $XO_3-O-C_3H_6$ formation scale linearly with one another with a slope of *ca.* 0.5 when the activation energy of $XO_3-O-C_3H_6$ formation is plotted against E_a for allylic-H abstraction (Figure 4A). From this, the most selective oxyanions for the first branching point are those with the highest E_a, which are also those with the highest pkB (see SI). Similarly, at the second branching point, E_a for PO formation is linearly correlated with E_a for PA formation with a slope of 0.7 (Figure 4B). This relationship again suggests that the oxyanions giving rise to the slowest rates are the most selective toward PO over silver.

While these scaling relationships show PO selectivity is maximized with nonbasic oxyanions, E_a associated with these species exceeds the *ca.* 1.1 eV associated with O_2 dissociation on Ag(111) on the low coverage limit.[9,10] The rapid combustion chemistry of O_{ads} would then be expected to dominate over that of the selective oxyanions. Thus, for simplicity, we can examine the oxyanions that show an activation energy equal to or lower than O_2 dissociation, since we know that barrier is crossed under experimental conditions relevant to epoxidation. When considering only those oxyanions with E_a below the O_2 dissociation barrier, we find that $SO_{4,ads}$ is surpassed in predicted PO selectivity by $SeO_{4,ads}$, which is predicted to produce PO selectively (Table S2).

An alternate strategy to avoid propylene combustions by O_{ads} would be to employ a more noble catalyst. Here, we computed the MEPs for the reactions of propylene with the two best oxyanions $SO_{4,ads}$ and $SeO_{4,ads}$ on Au(111) through the mechanism in Figure 1. While the scaling at each branching point remains unchanged from what was observed on Ag(111), the predicted maximum selectivity is lower than on Ag(111) owing to the lower E_a's on Au(111) (Figure 4A). An ideal catalyst/co-catalyst system would then be one with little O_{nuc} formation and weakly basic oxyanions, though such systems may require a second co-catalyst (such as Cl) to mediate $XO_{4,ads}$ coverage.

CONCLUSIONS

Our findings show that $SO_{4,ads}$ improves PO selectivity during gas-phase propylene partial oxidation over silver and can be activated by Cl. By bringing together the initial interpretation of the differences between propylene and ethylene epoxidation[11] with the recent findings on the nature of O_{elec},[9] we were able to design means of increasing PO selectivity during the direct partial oxidation of propylene over silver by more than 400%. We show the naturally present (SO_4) selective species does not form spontaneously during propylene oxidation on silver. We show O_{elec} can be increased by forming an inactive form that can be activated by Cl to produce the active $SO_{4,ads}$. We go on to show how different catalyst/co-catalysts systems can be used to further tune PO selectivity by rational design.

METHODS

Sample Preparation. Samples were prepared using high purity Ag powder (Alfa Aesar, 99.999%), 22 mesh. A total of 120 mg of Ag powder was pressed into an 8 mm diameter pellet using 0.2 ton, for 1 min.

***Operando* X-ray Photoelectron Spectroscopy (XPS).** The experiments were carried out at the synchrotron BESSY II near ambient pressure (NAP) XPS end station at the Innovative Station for In Situ Spectroscopy (ISISS) beamline and at the UE56/2 PGM-1 (BElChem) beamline, using a differentially pumped hemispherical analyzer Phoibus 150 from Specs GmbH. Appropriate photon energies were selected in order to measure the core-level spectra for all the elements with photoelectrons with the same kinetic energy (220 eV), providing a probing depth of approximately 6 Å. The NAP-XPS chamber consists of a (approximately) 10 L reaction cell. The sample was mounted into the (backfilled) reaction cell and heated from the back side using an infrared (IR) laser system. The temperature was measured using a thermocouple wire (Type K) pressed onto the sample surface. The IR laser power was monitored by a PID controller with temperature feedback. The gas mixtures were introduced into the reaction cell using mass flow controllers. For all experiments, the total flow was kept at 6 mL/min and the total pressure was set to 0.5 mbar. The reaction products were analyzed online by using quadrupole mass spectrometry (QMS) and/or gas chromatography (GC). A schematic representation of the setup arrangement is shown in Figure S1.

https://doi.org/10.1021/acscatal.3c00297
ACS Catal. 2023, 13, 5906−5913

Gas Chromatography and Quadrupole Mass Spectrometry. For some of the experiments, the detection of products was done by means of online gas chromatography (GC), Varian Micro-GC 4900, equipped with a PPQ column with heated injector. The GC equipment was installed at the outgoing flowing gas of the reaction chamber (Figure S1). The outgoing gas was continuously sampled by the GC every *ca.* 6 min. For the reaction, the sample was always a Ag pellet in O_2:C_3H_6 reaction mixture with a total flow of 6 mL/min into and out of the reaction cell kept at a constant 0.5 mbar total pressure. From all experiments, the main products were identified as CO_2 and propylene oxide (PO). This was done by using certified gas calibration mixtures containing CO_2 and PO. The calibration gases used consisted in 500 ppm PO in He (by Linde) and 2% CO_2 + 2% O_2 in N_2 (by Westfallen) (see Figure S3).

Mass Spectra were acquired online with a QMS (Pfeiffer Prisma) directly attached to the NAP-XPS chamber. The reaction chamber gas mixture was constantly introduced to the differentially pumped QMS via a leak valve (Figure S1). The pressure inside the QMS was set to 10^{-6} mbar. The possible products considered, and the corresponding mass fragments were chosen according to our previous GC results and literature reports.[1] The main products identified by GC, CO_2, PO, and H_2O were followed with QMS by acquiring the mass fragments m/z 44, m/z 58, and m/z 18, respectively.[1] Mass fragments of other common partial products reported to be detected in the literature (however, under different reaction conditions), such as acetone and acrolein,[1] were also monitored by acquiring the mass fragments m/z 43 and m/z 56, respectively. To identify product formation, all the corresponding mass fragments where continuously acquired during a temperature ramp from room temperature up to 270 °C (Figure S4) for all the different reaction mixtures (as indicated in the figure). From the QMS data, the main detected products in all cases were CO_2, H_2O, and PO, in agreement with the GC results. To ensure all detected products were being formed on the Ag sample, a blank-test reaction was performed by heating a sample holder (without sample) in the reaction mixture. No product formation was detected during the blank-test reaction without sample.

Dosing of SO_2 and C_2H_5Cl to the Reaction Feed. Small amounts of SO_2 and C_2H_5Cl were dosed using two independent leak valves directly attached to the NAP-XPS reaction chamber (Figure S1). For this, we used 1000 ppm SO_2 in He and 1%C_2H_5Cl in He.

Computational Methods. All DFT calculations were performed with the Quantum ESPRESSO package following the approach in ref 32. In brief, calculations were performed using the PBE exchange and correlation potential with PAW datasets from the PS library[33] with kinetic energy and charge density cutoffs of 30 and 300 Ry, respectively. Dispersion interactions were treated with the exchange-hole dipole moment (XDM).[34,35] Ag(111) surfaces were modeled using five-layer Ag slabs separated by *ca.* 15 Å vacuum and a k-point mesh equivalent to (12 × 12) for the (1 × 1) surface unit cell with cold smearing using a smearing parameter of 0.02 Ry.[36] All MEPs were computed using (4 × 4) surfaces with the climbing image nudged elastic band method using 8−16 images for each elementary step.

Figure S7 shows the MEP for the reaction of propylene with $SO_{3,ads}$. Figures S8 and S9 show the MEP for propylene reaction with O_{ads} (ally-H abstraction vs SO_2−O−C_3H_6 pathway) and the MEP for the partial oxidation pathway to PO and PA, respectively.

■ ASSOCIATED CONTENT

Supporting Information

The Supporting Information is available free of charge at https://pubs.acs.org/doi/10.1021/acscatal.3c00297.

Additional experimental details, setup details, additional spectra, calibration data, and additional calculations (PDF)

■ AUTHOR INFORMATION

Corresponding Authors

Emilia A. Carbonio − *Catalysis for Energy, CE-GKAT, Energy Materials In-situ Laboratory (EMIL), BESSY II, Helmholtz-Zentrum Berlin für Materialien und Energie GmbH, 12489 Berlin, Germany; Department of Inorganic Chemistry, Fritz-Haber-Institut der Max-Planck-Gesellschaft, 14195 Berlin, Germany;* orcid.org/0000-0003-2928-4599; Email: carbonio@fhi-berlin.mpg.de, emilia.carbonio@helmholtz-berlin.de

Travis E. Jones − *Department of Inorganic Chemistry, Fritz-Haber-Institut der Max-Planck-Gesellschaft, 14195 Berlin, Germany; Theoretical Division, Los Alamos National Lab, Los Alamos, New Mexico 00000, United States;* orcid.org/0000-0001-8921-7641; Email: tejones@lanl.gov

Authors

Frederic Sulzmann − *Department of Inorganic Chemistry, Fritz-Haber-Institut der Max-Planck-Gesellschaft, 14195 Berlin, Germany*

Alexander Yu. Klyushin − *Catalysis for Energy, CE-GKAT, Energy Materials In-situ Laboratory (EMIL), BESSY II, Helmholtz-Zentrum Berlin für Materialien und Energie GmbH, 12489 Berlin, Germany; Department of Inorganic Chemistry, Fritz-Haber-Institut der Max-Planck-Gesellschaft, 14195 Berlin, Germany;* Present Address: MAX IV Laboratory, Lund University, Box 118, 221 00 Lund, Sweden; orcid.org/0000-0003-1305-6911

Michael Hävecker − *Catalysis for Energy, CE-GKAT, Energy Materials In-situ Laboratory (EMIL), BESSY II, Helmholtz-Zentrum Berlin für Materialien und Energie GmbH, 12489 Berlin, Germany; Department of Heterogeneous Reactions, Max Planck Institute for Chemical Energy Conversion, Mülheim an der Ruhr 45470, Germany*

Simone Piccinin − *CNR-IOM DEMOCRITOS, Consiglio Nazionale delle Ricerche—Istituto Officina dei Materiali, 34136 Trieste, Italy;* orcid.org/0000-0002-3601-7141

Axel Knop-Gericke − *Department of Inorganic Chemistry, Fritz-Haber-Institut der Max-Planck-Gesellschaft, 14195 Berlin, Germany; Department of Heterogeneous Reactions, Max Planck Institute for Chemical Energy Conversion, Mülheim an der Ruhr 45470, Germany*

Robert Schlögl − *Department of Inorganic Chemistry, Fritz-Haber-Institut der Max-Planck-Gesellschaft, 14195 Berlin, Germany; Department of Heterogeneous Reactions, Max Planck Institute for Chemical Energy Conversion, Mülheim an der Ruhr 45470, Germany*

Complete contact information is available at: https://pubs.acs.org/10.1021/acscatal.3c00297

https://doi.org/10.1021/acscatal.3c00297
ACS Catal. 2023, 13, 5906−5913

Notes

The authors declare no competing financial interest.

■ ACKNOWLEDGMENTS

We thank the Helmholtz-Zentrum Berlin for providing support of the in situ electron spectroscopy activities of the FHI at ISISS and UE56-PGM1 beamlines in BESSY II and the Max-Planck Gesellschaft for generous founding. We gratefully acknowledge Höchstleistungsrechenzentrum Stuttgart (HLRS) for generous access to the supercomputer HazelHen through the SEES2 project. T.J. acknowledges support from the US DOE, Office of Science, Basic Energy Sciences, Chemical Sciences, Geosciences, and Biosciences Division under Triad National Security, LLC ("Triad") contract grant 89233218CNA000001 (FWP: LANLE3F2). Open Access funding has been enabled and organized by Helmholtz-Zentrum Berlin für Materialien und Energie.

■ ABBREVIATIONS

EO, ethylene oxide; PO, propylene oxide; MEP, minimum energy path; DFT, density functional theory; XPS, X-ray photoelectron spectroscopy

■ REFERENCES

(1) Lei, Y.; Mehmood, F.; Lee, S.; Greeley, J.; Lee, B.; Seifert, S.; Winans, R. E.; Elam, J. W.; Meyer, R. J.; Redfern, P. C.; Teschner, D.; Schlogl, R.; Pellin, M. J.; Curtiss, L. A.; Vajda, S. Increased Silver Activity for Direct Propylene Epoxidation via Subnanometer Size Effects. *Science* **2010**, *328*, 224−228.

(2) Khatib, S. J.; Oyama, S. T. Direct Oxidation of Propylene to Propylene Oxide with Molecular Oxygen: A Review. *Catalysis Reviews* **2015**, *57*, 306−344.

(3) Marimuthu, A.; Zhang, J.; Linic, S. Tuning Selectivity in Propylene Epoxidation by Plasmon Mediated Photo-Switching of Cu Oxidation State. *Science* **2013**, *339*, 1590−1593.

(4) Baer, H., Bergamo, M., Forlin, A., Pottenger, L. H, Lindner, J., Propylene Oxide. In *Ullmann's Encyclopedia of Industrial Chemistry*. Wiley-VCH Verlag GmbH & Co KGaA: Weinheim, 2012.

(5) Monnier, J. R., The selective epoxidation of non-allylic olefins over supported silver catalysts. In *Studies in Surface Science and Catalysis*, Grasselli, R. K.; Oyama, S. T.; Gaffney, A. M.; Lyons, J. E., Eds. Elsevier: 1997; Vol. *110*, pp. 135−149.

(6) Isegawa, K.; Ueda, K.; Hiwasa, S.; Amemiya, K.; Mase, K.; Kondoh, H. Formation of Carbonate on Ag(111) under Exposure to Ethylene and Oxygen Gases Evidenced by Near Ambient Pressure XPS and NEXAFS. *Chem. Lett.* **2019**, *48*, 159−162.

(7) Jones, T. E.; Rocha, T. C. R.; Knop-Gericke, A.; Stampfl, C.; Schlogl, R.; Piccinin, S. Insights into the Electronic Structure of the Oxygen Species Active in Alkene Epoxidation on Silver. *ACS Catal.* **2015**, *5*, 5846−5850.

(8) Bukhtiyarov, V. I.; Prosvirin, I. P.; Kvon, R. I. Study of Reactivity of Oxygen States Adsorbed at a Silver Surface Towards C2h4 by Xps Tpd and Tpr. *Surf. Sci.* **1994**, *320*, L47−L50.

(9) Jones, T. E.; Wyrwich, R.; Bocklein, S.; Carbonio, E. A.; Greiner, M. T.; Klyushin, A. Y.; Moritz, W.; Locatelli, A.; Mentes, T. O.; Nino, M. A.; Knop-Gericke, A.; Schlogl, R.; Gunther, S.; Wintterlin, J.; Piccinin, S. The Selective Species in Ethylene Epoxidation on Silver. *ACS Catal.* **2018**, *8*, 3844−3852.

(10) Jones, T. E.; Wyrwich, R.; Bocklein, S.; Rocha, T. C. R.; Carbonio, E. A.; Knop-Gericke, A.; Schlogl, R.; Gunther, S.; Wintterlin, J.; Piccinin, S. Oxidation of Ethylene on Oxygen Reconstructed Silver Surfaces. *J. Phys. Chem. C* **2016**, *120*, 28630−28638.

(11) Palermo, A.; Husain, A.; Tikhov, M. S.; Lambert, R. M. Ag-Catalysed Epoxidation of Propene and Ethene: An Investigation Using Electrochemical Promotion of the Effects of Alkali, NOX, and Chlorine. *J. Catal.* **2002**, *207*, 331−340.

(12) Pu, T.; Tian, H.; Ford, M. E.; Rangarajan, S.; Wachs, I. E. Overview of Selective Oxidation of Ethylene to Ethylene Oxide by Ag Catalysts. *ACS Catal.* **2019**, *9*, 10727−10750.

(13) Carbonio, E. A.; Rocha, T. C. R.; Klyushin, A. Y.; Pis, I.; Magnano, E.; Nappini, S.; Piccinin, S.; Knop-Gericke, A.; Schlogl, R.; Jones, T. E. Are multiple oxygen species selective in ethylene epoxidation on silver? *Chem. Sci.* **2018**, *9*, 990−998.

(14) Isegawa, K.; Ueda, K.; Amemiya, K.; Mase, K.; Kondoh, H. Formation and Behavior of Carbonates on Ag(110) in the Presence of Ethylene and Oxygen. *J. Phys. Chem. C* **2021**, *125*, 9032−9037.

(15) Andryushechkin, B. V.; Shevlyuga, V. M.; Pavlova, T. V.; Zhidomirov, G. M.; Eltsov, K. N. STM and DFT Study of Chlorine Adsorption on the Ag(111)-p(4 x 4)-O Surface. *J. Phys. Chem. C* **2018**, *122*, 28862−28867.

(16) Van Santen, R. A.; Kuipers, H. P. C. E. The Mechanism of Ethylene Epoxidation. *Adv. Catal.* **1987**, *35*, 265−321.

(17) Sachtler, W. M. H.; Backx, C.; Vansanten, R. A. On the Mechanism of Ethylene Epoxidation. *Catal. Rev.: Sci. Eng.* **1981**, *23*, 127−149.

(18) Bukhtiyarov, V. I.; Knop-Gericke, A. Ethylene Epoxidation over Silver Catalysts. *Nanostruct. Catal.* **2011**, *19*, 214−247.

(19) Pulido, A.; Concepción, P.; Boronat, M.; Corma, A. Aerobic epoxidation of propene over silver (111) and (100) facet catalysts. *J. Catal.* **2012**, *292*, 138−147.

(20) Jones, T. E.; Rocha, T. C. R.; Knop-Gericke, A.; Stampfl, C.; Schlogl, R.; Piccinin, S. Thermodynamic and spectroscopic properties of oxygen on silver under an oxygen atmosphere. *Phys. Chem. Chem. Phys.* **2015**, *17*, 9288−9312.

(21) Wyrwich, R.; Jones, T. E.; Günther, S.; Moritz, W.; Ehrensperger, M.; Böcklein, S.; Zeller, P.; Lünser, A.; Locatelli, A.; Menteş, T. O.; Niño, M. Á.; Knop-Gericke, A.; Schlögl, R.; Piccinin, S.; Wintterlin, J. LEED-I(V) Structure Analysis of the $(7 \times \sqrt{3})$rect SO4 Phase on Ag(111): Precursor to the Active Species of the Ag-Catalyzed Ethylene Epoxidation. *J. Phys. Chem. C* **2018**, *122*, 26998−27004.

(22) Torres, D.; Lopez, N.; Illas, F.; Lambert, R. M. Low-basicity oxygen atoms: A key in the search for propylene epoxidation catalysts. *Angew. Chem. Int. Ed.* **2007**, *46*, 2055−2058.

(23) Barteau, M. A.; Madix, R. J. Low-Pressure Oxidation Mechanism and Reactivity of Propylene on Ag(110) and Relation to Gas-Phase Acidity. *J. Am. Chem. Soc.* **1983**, *105*, 344−349.

(24) Alemozafar, A. R.; Madix, R. J. Surface reorganization accompanying the formation of sulfite and sulfate by reaction of sulfur dioxide with oxygen on Ag(111). *J Chem Phys* **2005**, *122*, 214718.

(25) Rocha, T. C. R.; Havecker, M.; Knop-Gericke, A.; Schlogl, R. Promoters in heterogeneous catalysis: The role of Cl on ethylene epoxidation over Ag. *J. Catal.* **2014**, *312*, 12−16.

(26) Zimmermann, H., Propene. In *Ullmann's Encyclopedia of Industrial Chemistry*, Wiley-VCH Verlag GmbH & Co. KGaA, 2013.

(27) Frank, E. R.; Hamers, R. J. Chlorine-Induced Restructuring of Ag(111) Films Observed by Scanning Tunneling Microscopy. *J. Catal.* **1997**, *172*, 406−413.

(28) Andryushechkin, B. V.; Cherkez, V. V.; Gladchenko, E. V.; Zhidomirov, G. M.; Kierren, B.; Fagot-Revurat, Y.; Malterre, D.; Eltsov, K. N. Atomic structure of Ag(111) saturated with chlorine: Formation of Ag_3Cl_7 clusters. *Phys. Rev. B* **2011**, *84*, No. 075452.

(29) Andryushechkin, B. V.; Cherkez, V. V.; Gladchenko, E. V.; Zhidomirov, G. M.; Kierren, B.; Fagot-Revurat, Y.; Malterre, D.; Eltsov, K. N. Structure of chlorine on Ag(111): Evidence of the (3x3) reconstruction. *Phys. Rev. B* **2010**, *81*, No. 205434.

(30) Van den Reijen, J. E.; Kanungo, S.; Welling, T. A. J.; Versluijs-Helder, M.; Nijhuis, T. A.; de Jong, K. P.; de Jongh, P. E. Preparation and particle size effects of Ag/α-Al_2O_3 catalysts for ethylene epoxidation. *J. Catal.* **2017**, *356*, 65−74.

https://doi.org/10.1021/acscatal.3c00297
ACS Catal. 2023, 13, 5906−5913

(31) Campbell, C. T.; Koel, B. E. Chlorine promotion of selective ethylene oxidation over Ag(110): Kinetics and mechanism. *J. Catal.* **1985**, *92*, 272−283.
(32) Giannozzi, P.; Baroni, S.; Bonini, N.; Calandra, M.; Car, R.; Cavazzoni, C.; Ceresoli, D.; Chiarotti, G. L.; Cococcioni, M.; Dabo, I.; Dal Corso, A.; de Gironcoli, S.; Fabris, S.; Fratesi, G.; Gebauer, R.; Gerstmann, U.; Gougoussis, C.; Kokalj, A.; Lazzeri, M.; Martin-Samos, L.; Marzari, N.; Mauri, F.; Mazzarello, R.; Paolini, S.; Pasquarello, A.; Paulatto, L.; Sbraccia, C.; Scandolo, S.; Sclauzero, G.; Seitsonen, A. P.; Smogunov, A.; Umari, P.; Wentzcovitch, R. M. QUANTUM ESPRESSO: a modular and open-source software project for quantum simulations of materials. *J. Phys.: Condens. Matter* **2009**, *21*, No. 395502.
(33) Dal Corso, A. Pseudopotentials periodic table: From H to Pu. *Comput. Mater. Sci.* **2014**, *95*, 337−350.
(34) Becke, A. D.; Johnson, E. R. Exchange-hole dipole moment and the dispersion interaction revisited. *J. Chem. Phys.* **2007**, *127*, 154108.
(35) Otero-de-la-Roza, A.; Johnson, E. R. Van der Waals interactions in solids using the exchange-hole dipole moment model. *J. Chem. Phys.* **2012**, *136*, 174109.
(36) Marzari, N.; Vanderbilt, D.; De Vita, A.; Payne, M. C. Thermal contraction and disordering of the Al(110) surface. *Phys. Rev. Lett.* **1999**, *82*, 3296−3299.

https://doi.org/10.1021/acscatal.3c00297
ACS Catal. 2023, 13, 5906−5913